Annealing Effects of Dilute Polyaniline/NMP Solution

Young Moo Lee,* Jae Hoon Kim, Jong Seok Kang, and Seong Yong Ha

School of Chemical Engineering, College of Engineering, Hanyang University, Seoul 133-791, Korea

Received November 30, 1999; Revised Manuscript Received August 3, 2000

ABSTRACT: The annealing effects of a dilute polyaniline solution on chemical and physical properties were investigated. Emeraldine base (EB) of polyaniline prepared by the conventional procedure was dissolved in 1-methyl-2-pyrrolidinone (NMP). After heating at 60−140 °C for 2 h, the color of PANi solution changed from deep blue to various colors depending on the annealing temperature. This solution was filtered and cooled at −5 °C to preserve an undoped structure. Changes of physical and chemical properties were investigated using ultraviolet−visible (UV−vis), Fourier transform infrared (FT-IR) spectroscopy, electron spectroscopy for chemical analysis (ESCA), and dynamic light scattering (DLS). By contrast to the previously reported reductive reaction, we concluded that the annealing of dilute EB/NMP solution resulted in cross-linking. This was indicated by the decrease of the mutual diffusion coefficient at infinite dilution (D_0) and the increase in the apparent hydrodynamic radius (R_h) of EB with the annealing temperature evidenced by the DLS and the increase of the cyclic-N portion from ESCA results. The annealing also produces a polyelectrolyte chain, supported by FT−IR and DLS measurements.

1. Introduction

Conducting polymers, e.g., polyacetylene, polypyrrole, polythiophene, and polyaniline, etc., have been of special interest in recent decades. Among these polymers, polyaniline (PANi) has attracted a considerable scientific attention because of its electronic and photonic states as well as high conductivities and environmental stabilities.[1−3] PANi can be synthesized by oxidation polymerization. Depending on its oxidation states and doping processes, PANi has four forms (see Figure 1); fully oxidized pernigraniline, half-oxidized emeraldine base (EB), fully reduced leucoemeraldine base (LB), and metallic emeraldine salt. The conducting form of PANi (emeraldine salt) powder synthesized in aqueous HCl solution is insoluble in most common organic solvents including 1-methyl-2-pyrrolidinone (NMP). However, EB, which can be obtained by treating emeraldine salt with aqueous NH_4Cl solution, is soluble in NMP and can be cast into film from EB/NMP solution.[4,5]

Although the thermal properties of PANi have been reported in recent years, little is known on annealing effects, particularly of PANi in its solution state. MacDiarmid et al. reported that the cross-linking reaction occurred when EB powder was heated to 300 °C. Chen et al. reported changes of physical properties of EB annealed at 150−300 °C, i.e., the peak at 1589 cm^{-1} (N═Q═N stretching, Q = quinoid ring) disappeared, and the peak at 1496 cm^{-1} (N−B−N stretching, B = benzenoid ring) increased in IR spectra.[7] Conklin et al. also reported that the solubility of annealed EB powder in NMP was significantly reduced and that the cross-linking reaction between EB chains reduced the conjugation length as shown by the blue shift of UV−vis spectra. Moreover, they mentioned that after annealing the free electron concentration increased up to 10-fold compared with nonannealed PANi.[8] As for the thermal properties of PANi in its solution state, Afzali et al. reported that PANi in NMP solution is reduced at 160−180 °C to its LB form.[9] They suggested that a reduction instead of the cross-linking reaction occurred, because the peak retention time in gel permeation chromatography (GPC) changed little by the heat treatment and the imine nitrogen XPS peak almost disappeared when PANi/NMP was heated.

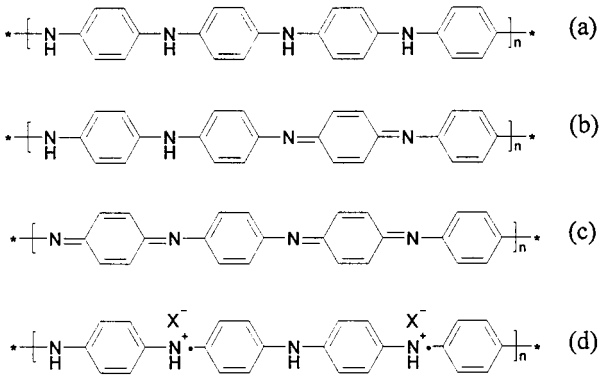

Figure 1. Four forms of PANi: (a) leucoemeraldine base; (b) emeraldine base; (c) permigraniline base; (d) metallic emeraldine salt.

In this article, we present a study of annealing effects in dilute PANi (EB)/NMP solution at temperatures up to 140 °C. The physical and chemical changes and the detailed mechanism of annealed EB solutions were monitored by Fourier transform infrared (FT-IR), ultraviolet−visible (UV−vis) spectroscopy, electron spectroscopy for chemical analysis (ESCA), and dynamic light scattering (DLS). One of the problems in investigating the solution properties of PANi using DLS is its absorption of light, and thus we narrow the concentration range to very dilute solutions (0.02 mg/mL).

2. Experimental Section

Materials. Aniline (Yakuri Pure Chemical) was dried with CaH_2 and distilled at reduced pressure. Ammonium persulfate ($(NH_4)_2S_2O_8$, Junsei Chemical; minimum assay 95%) was used without further purification. 1-Methy-2−pyrrolidinone (NMP, Aldrich, minimum assay 99.5%) was used as a solvent without purification.

Preparation of PANi/NMP Solutions. PANi (EB) was prepared following the method of MacDiarmid et al.[10] The

* Corresponding author. Tel +82-2-2291-9683; Fax +82-2-2291-5982; E-mail ymlee@email.hanyang.ac.kr.

10.1021/ma992004y CCC: $19.00
Published on Web 09/14/2000

detailed procedure was previously reported.[11] The weight-average molecular weight of EB, determined by static light scattering method, was 230 000.[11] The annealing was carried out using EB/NMP solution (0.02 mg/mL) under a nitrogen stream. After 2 h of heating at 60, 80, 100, 120, and 140 °C, the solution was cooled and filtered using a 0.2 μm Millipore syringe filter.

Characterization. a. UV−vis. To investigate the optical properties of the annealed solutions, UV−vis absorption spectra were recorded on HP 8452 A diode array spectrometer.

b. FT-IR. The infrared spectrum of EB powder and LB powder was obtained from a mixture of sample with KBr in pellet form. To prepare thin film of EB, 3 wt % EB/NMP solution was poured into a Petri dish and then dried at 45 °C in the vacuum oven. To obtain a thin film of the solution annealed at 140 °C, the NMP was distilled under vacuum so that about 3 wt % PANi/NMP was obtained. The concentrated solutions were poured into a Petri dish and then dried at 45 °C in the vacuum oven. The residual NMP in the film and in the annealed film were further removed by methanol extraction. All the samples were kept under a nitrogen atmosphere before the analysis by Fourier transform infrared (FT-IR, Nicolet model Magna IR 550, Madison, WI).

c. ESCA. The changes in chemical structure of the annealed solutions were analyzed by electron spectroscopy for chemical analysis (ESCA, Omicron EA125, Philadelphia, PA) using Mg Kα source at 1253.6 eV and 300 W power at the anode. The pressure in the chamber was maintained under 10^{-9} mbar or lower during the measurement. The sample position and tilt angle (30° for narrow scan) were fine-tuned for optimal data acquisition. A thin film of annealed solution was obtained by the same manner as described in the FT-IR section. The ESCA data were analyzed with a least-squares fitting routine. All the binding energies were referenced to the C_{1s} neutral carbon peak at 284.8 ± 0.1 eV to compensate for surface charging effects.[12] In the peak deconvolution, experimental spectra are calculated by the best-fit contributions assuming 50% Lorentzian−Gaussian peaks and a Shirley background[13] over the energy range of the fit.

d. DLS. Dynamic light scattering was carried out on a Bookhaven Instruments Corporation package composed of a BI200SM goniometer, a BI9000AT correlator with the digital 8 bits × 256 channels (maximum), an EMI9863 photomultiplier for photon counting, an argon ion laser (Lesel Laser Inc., model 95-1) operated at 514.5 nm wavelength and 100 mW intensity, a thermostatic bath (temperature stability ±0.05 °C), and an associated software package for data analysis of DLS including single and double exponential, CUMULANT and CONTIN.[14] The scattering intensity was measured at 30°, 60°, 90°, 120°, and 150°. For DLS measurements, dilute solutions were prepared by direct addition of filtered NMP and the cells flame-sealed under mild vacuum. The resulting dilute PANi/NMP solutions were stable over time, showing the same correlation function weeks after initial measurement. The relaxation times obtained using CONTIN fell into two categories: a fast mode caused by molecular diffusion and a slow mode caused by internal mode. The mutual diffusion coefficients at infinite dilution, D_0, the concentration coefficient, k_D, and the apparent hydrodynamic radii, R_h, are evaluated.[15]

3. Results and Discussion

Ultraviolet−Visible (UV−vis) Spectroscopy. The UV−vis spectra of dilute PANi/NMP solutions with various annealing temperatures are shown in Figure 2. Up to 100 °C, the solutions showed the original blue color of EB with two characteristic peaks: exciton absorption of quinoid at ~640 nm and $\pi-\pi^*$ absorption peak of benzenoid rings at ~330 nm.[16,17] Above 120 °C, however, the color of the solution changed to yellow with an intense increase of the benzenoid peak at the expense of a decrease of quinoid rings. At least two possible effects can explain this phenomenon. First, EB was reduced to LB by the presence of NMP. In order for EB to be reduced, NMP must act as a donor of hydrogen atoms.[9] Second, a cross-linking reaction between quinoid rings and the imine nitrogen may have occurred.

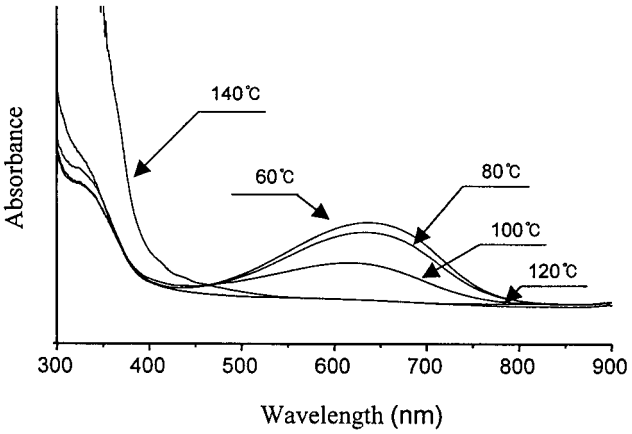

Figure 2. UV−vis absorption spectra of EB/NMP solution with annealing temperature.

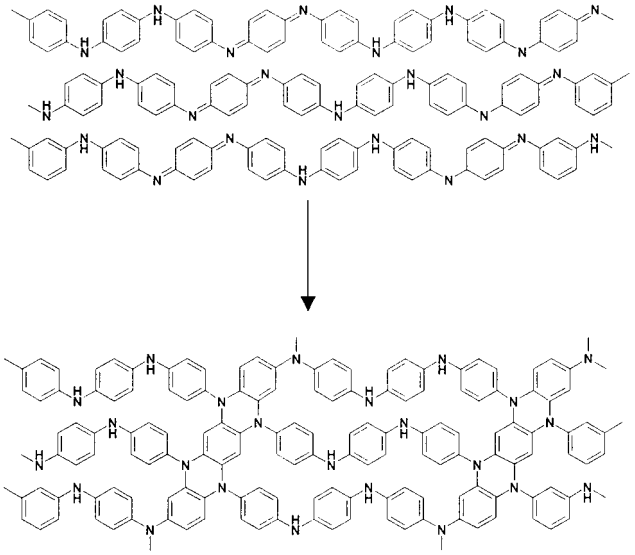

Figure 3. Proposed cross-linking scheme of PANi (EB).

Figure 3 shows a cross-linking scheme proposed by various groups.[5−7] To oxidize yellow EB/NMP solutions that were annealed above 120 °C, various oxidants such as bubbling oxygen, H_2O_2, PbO_2, and APS were used.[18] In this study, the yellow color of the solution did not change to blue even after the addition of oxidants, which supported the cross-linking reaction instead of the reduction. The maximum absorbance of the exciton peak shifted from 641 to 615 nm after heating for 2 h at 100 °C. The blue shift caused by the shortening conjugation length for annealed EB is probably due to a cross-linking reaction[8] and/or a decreasing chain length of the EB upon heating, as will be discussed later.

Infrared Spectroscopy (IR). The FT-IR spectra of EB powder, EB film cast from a NMP solution, LB powder, 140 °C annealed EB/NMP film, and NMP are shown in Figure 4. The major characteristic peaks are summarized in Table 1. For the EB/NMP film, the absorption peak of the C═O stretching shifted by 12 cm^{-1} from 1682 (of pure NMP) to 1670 cm^{-1}. The C═O group of NMP formed a hydrogen bond with the amine site of EB, i.e., C═O· · ·N−H.[21] This is also consistent with the fact that there is no intense free N−H stretching peak in EB/NMP film. When NMP is removed by

Table 1. Characteristic Peaks (cm^{-1}) of the IR Spectra of Polyanilines[a]

assignment[b]	EB powder	EB/NMP film	EB/NMP film after MeOH extraction	140 °C annealed EB/NMP film after MeOH extraction	LB powder	NMP
str of free N−H	3385	3376	3385	disappeared	3376	
str of H-bonded N−H	3293	3295	3292	disappeared		
str of methyl C−H				2921		2944
str of methylene C−H				2846		2877
str of C═O		1670	disappeared	1657		1682
str of N═Q═N	1590	1595	1595	disappeared	1595	
str of N═B═N	1502	1508	1502	1508	1500	
sci of methylene C−H				1462		1464
ben of methyl C−H				1363		1400
str of C−N (QB^tQ)	1379	1381	1379	disappeared		
str of C−N (QB^cQ, QBB, BBQ)	1311	1309	1311	disappeared	1282	1298
str of C−N (BBB)	1235	1232	1235	1232		
a mode of N═Q═N	1160	1167	1167	disappeared		
ben of $C_{aromatic}$−H	836	834	825	842	813	

[a] From refs 19 and 20. [b] str = stretching; ben = bending; sci = scissoring; Q = quinoid unit; B = benzenoid unit; Bt = trans benzenoid unit; Bc = cis benzenoid unit.

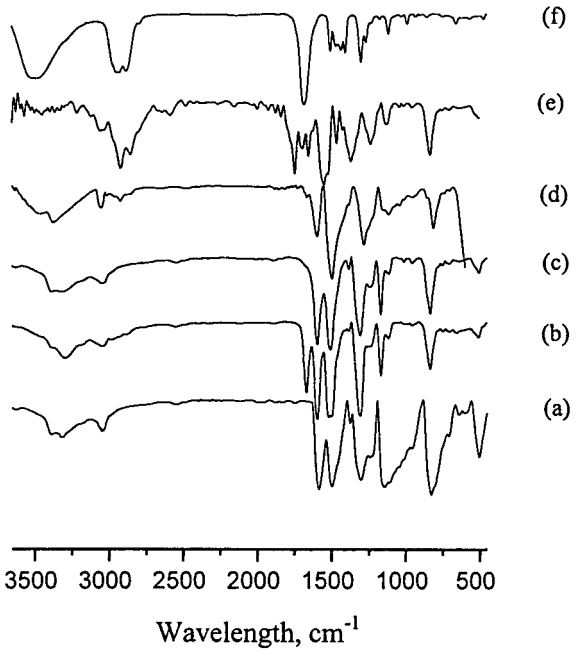

Figure 4. FT-IR spectra of (a) EB powder, (b) EB/NMP film, (c) EB/NMP film after methanol extraction, (d) LB powder, (e) 140 °C annealed EB/NMP film after methanol extraction, and (f) NMP.

methanol extraction, the C═O peak completely disappears and free N−H stretching peak appears at 3386 cm^{-1} (see Figure 4b,c). When comparing the EB/NMP film annealed at 140 °C after methanol extraction with the EB/NMP unannealed film after methanol extraction, at least two major changes can be noticed. First, the absorption peaks related to the quinoid ring (1595, 1381, 1309 cm^{-1}) disappeared, which was consistent with the result of UV−vis. Second, the N−H stretching peaks at 3300−3500 cm^{-1} disappeared, and the peaks related to methyl C−H and methylene C−H (2921, 2846, 1462, 1363 cm^{-1}) and C═O stretching at 1657 cm^{-1} newly appeared (see Table 1). Although we tried to remove NMP from the annealed film at 140 °C by methanol extraction (cf. Figure 4e), there was still a C═O stretching peak due to residual NMP. It was probably due to a charge-transfer complex formed by NMP and EB at the high annealing temperature, as will be discussed later.

Electron Spectroscopy for Chemical Analysis (ESCA). The changes of the atomic surface composition in the annealed PANi were further determined by ESCA analysis. In general, PANi contains quinoid imine and benzenoid amine units, and the oxidation state of PANi can be characterized by the relative amount of these units from the fully oxidized pernigraniline to fully reduced leucoemeraldine base. The half-oxidation state of the emeraldine base has an approximately an equal amount of amine and imine nitrogens.

Figure 5 shows the characteristic high-resolution C_{1s} and N_{1s} spectra of an EB film cast from a NMP solution and an EB/NMP film annealed at 140 °C after methanol extraction. The EB film surface was smoothly fitted into four carbon peaks: aromatic carbon (−C_{Ar}) at the binding energy of 284.8 ± 0.1 eV, carbon atom with a single bond to nitrogen (−C−N) at 285.5 ± 0.1 eV, carbon atom with double bonds to nitrogen (−C═N) at 286.2 ± 0.1 eV, and a low-intensity component at ∼289.3 eV.[22] This high tail in the C_{1s} core level spectrum is poorly defined; it has been attributed to the residual NMP in the film, surface oxidation product, weakly charge-transfer complexed oxygen on the EB film, or a shake-up satellite.[23−25] We attributed this peak to a shake-up satellite because the residual NMP in the sample was removed completely by methanol extraction as confirmed by FT-IR when the sample was kept under the nitrogen before mounting in the analysis chamber. The annealed EB/NMP surface showed new peaks at higher binding energies, indicating the formation of carbon−oxygen double bonds (−C═O, carbonyl carbon) at 287.9 ± 0.1 eV.[26,27] This is consistent with the FT-IR results; unlike EB/NMP film, it was not possible to remove the residual NMP in the EB/NMP film annealed at 140 °C by methanol extraction. The N_{1s} spectra were fitted into four component peaks: imine nitrogen (N═C−) at 398.1 ± 0.1 eV, amine nitrogen (−N−C−) at 399.3 ± 0.1 eV, cyclic nitrogen (−N═) at 401.3 ± 0.1 eV, and imine shake-up at 403.0 ± 0.1 eV.[28−30] The N_{1s} spectrum of LB exhibits only a single nitrogen environment at about 399.3 eV, which is characteristic of the amine nitrogen.[31] Table 2 summarizes the results from the peak fitting of ESCA C_{1S} and N_{1s} spectra for the EB/NMP film and 140 °C annealed EB/NMP film. It should be noted that our ESCA result and that of other work groups[22,28−30] indicate more amine than imine, albeit the EB state is often described as half amine and half imine. The following tendencies had been observed; the imine-to-amine ratio changed from 0.58 at room temperature to about 0.22 after annealing at 140 °C for

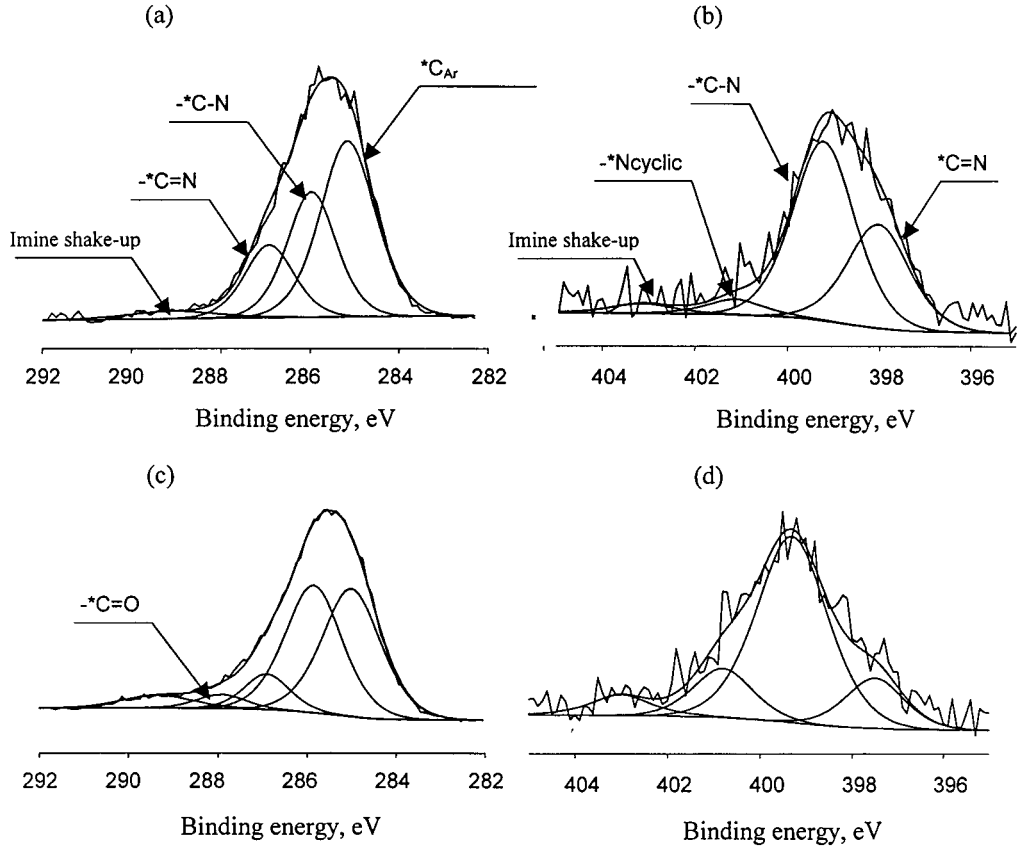

Figure 5. High-resolution ESCA C 1s core level spectra of (a) EB/NMP film after methanol extraction, (b) 140 °C annealed EB/NMP film after methanol extraction, N 1s core level spectra of (c) EB/NMP film after methanol extraction, and (d) 140 °C annealed EB/NMP film after methanol extraction.

Table 2. ESCA Analysis of Polyanilines

	atomic % of C_{1s} or N_{1s} spectra[a]	
sample	unannealed EB/NMP film	140 °C annealed EB/NMP film
aromatic (−*C−C) 284.8 ± 0.1 eV	48.1	41.6
amine (−*C−N−) 285.5 ± 0.1 eV	30.6	40.4
imine (−*C=N) 286.2 ± 0.1 eV	17.8	9.0
carbonyl (−*C=O) 287.9 ± 0.1 eV		3.8
imine (*N=C−) 398.1 ± 0.1 eV	33.7	14.5
amine (−*N−C−) 399.3 ± 0.1 eV	58.0	64.8
cyclic (−*N=) 401.3 ± 0.1 eV	4.9	14.2
imine shake-up 403.0 ± 0.1 eV	3.4	6.5

[a] The asterisk corresponds to the analyzed carbon and nitrogen.

2 h, which was in a good agreement with N_{1s} results. This reduction in this ratio can be attributed to the cross-linking reaction; the nitrogen attached to the quinoid ring attacked neighboring quinoid rings, resulting in two benzenoid rings and two cyclic nitrogen, as suggested by Scheer et al.[6] The amount of cyclic nitrogen, which appeared in place of imine nitrogen, increased to 14.2% upon exposure at high temperature, indicating a cross-linking reaction caused by the annealing process (see Figure 3). Moreover, the increment of the shake-up satellite may be attributed to a more localized electronic structure,[32,33] consistent with a loss of conjugation.[25] Thus, the ESCA data are consistent with the UV−vis and FT-IR data.

Dynamic Light Scattering (DLS). The normalized intensity correlation function, $g^{(1)}(t)$, of scattered light of EB/NMP solution exhibits a single relaxation curve at all scattering angles θ in the decay time range of $1-10^6$ μs. A representative set of data are shown in Figure 6a measured at θ = 30°, 90°, and 150°. In general, NMP is not a good solvent for EB because of the strong hydrogen bonding between amine and imine nitrogen atoms in the EB backbone.[34,35] For example, EB chains form aggregates in NMP solution as evidenced by a bimodal molecular weight distribution of EB chains based on the gel permeation chromatography data.[36,37] The aggregation of the EB chain in NMP has been detected by DLS as well as by GPC; it has been reported that dilute EB/NMP solutions have two relaxation modes, a fast mode and a slow mode.[38,39] A fast relaxation mode is attributed to the diffusion of a single polymer chain while a slow mode is due to large particles or aggregates,[40,41] complexation,[42] or gelation[43,44] by (physical or chemical) cross-linking in the dilute regime. In the case of EB/NMP solutions, the slow mode corresponds to the peak related to the high molecular weight compounds confirmed by many GPC studies, as mentioned before. However, the relative percentage of aggregation of EB in NMP is highly dependent on the concentration of polymer solution. As the concentration of polymer decreases in a given solvent, the solvent−polymer interaction increases while the polymer−polymer interaction decreases. The sample prepared in this study was very dilute (0.02 mg/mL) enough to exhibit only one decay process. CONTIN analysis was then applied for an estimation of Γ as a quantity characteristic of the diffusion behavior of EB in dilute solution.

By contrast, Figure 6b depicts the normalized intensity correlation function at a series of the scattering vector for the EB/NMP solution annealed at 140 °C. As we increased the scattering vector, a slow mode appeared. These relaxation times were analyzed by CON-

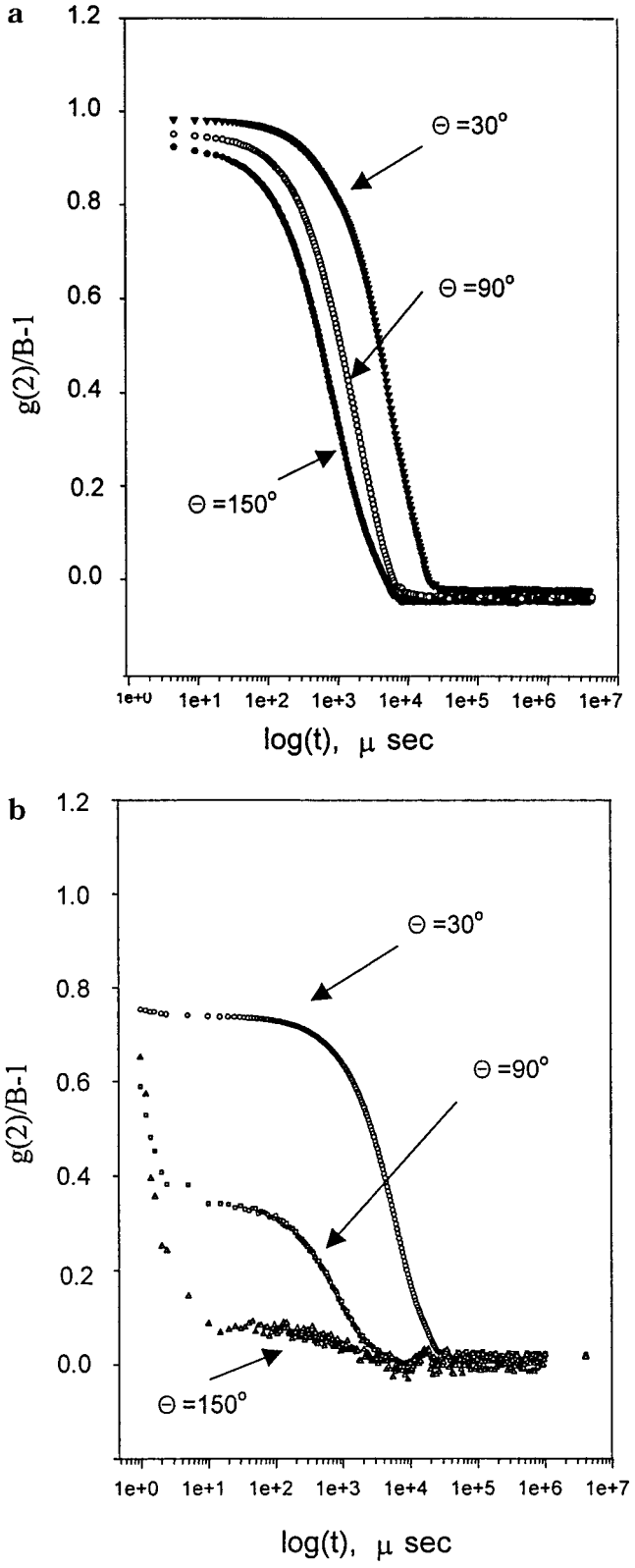

Figure 6. (a) Time profile of the normalized intensity correlation function, $g^{(1)}(t)$, of light intensity scattered from the nonannealed EB/NMP solution at the scattering angle 30°, 90°, and 150°; $C = 0.02$ mg/mL, $T = 25$ °C. (b) Time profile of the normalized intensity correlation function, $g^{(1)}(t)$, of light intensity scattered from the 140 °C annealed EB/NMP solution at the scattering angle 30°, 90°, and 150°; $C = 0.02$ mg/mL, $T = 25$ °C.

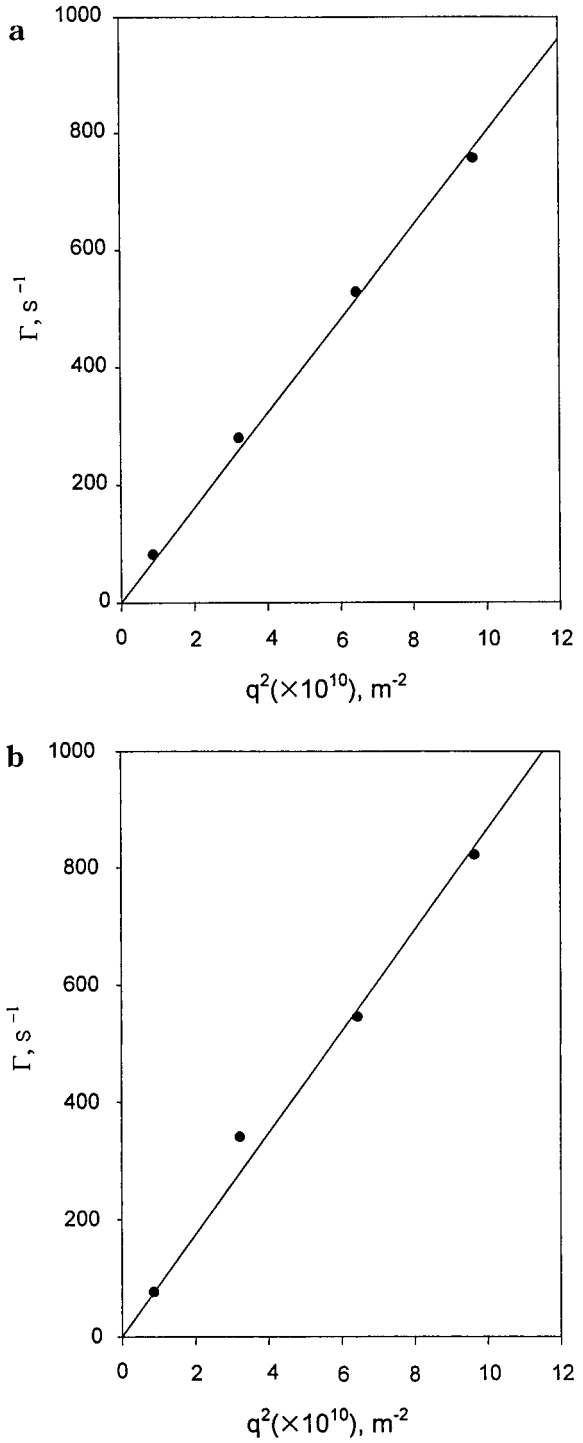

Figure 7. (a) Dependence of the decay rate, Γ, on the magnitude q^2 of the scattering vector for a dilute EB/NMP solution ($C = 0.02$ mg/mL); filled point were resulted from CONTIN; solid line from the linear fit. (b) Dependence of the decay rate, Γ_s, of the slow mode on the magnitude q^2 of the scattering vector for a dilute 140 °C annealed EB/NMP solution ($C = 0.02$ mg/mL); filled point were resulted from CONTIN; solid line from the linear fit.

TIN. The decay rate, Γ, characteristic of the slow mode showed a linear dependence of q^2. This result indicates that the slow mode is the diffusive mode, and the mutual diffusion coefficient, $D_m = \Gamma/q^2$, can be estimated using the slope obtained through linear regression analysis (Figure 7). The dependence of D_m on the polymer concentration is shown in Figure 8 for four samples. Mutual diffusion coefficients at infinite dilution, D_0, and diffusional second virial coefficients, k_d, are obtained by linear regression analysis and listed in Table 3 (cf. eq 7). In general, D_0 is interpreted as the

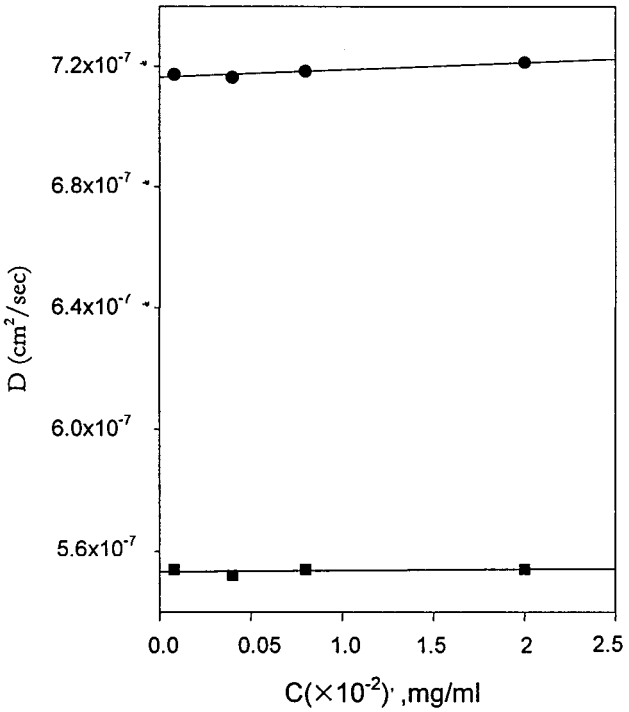

Figure 8. Extrapolation of the mutual diffusion coefficient, D_m, to measure the mutual diffusion coefficient at infinite dilution, D_0, and the diffusional second virial coefficient, k_d, for (●) EB/NMP and (■) 140 °C annealed EB/NMP solutions in different concentration.

Table 3. Experimental Result of D_0 and k_d

	M_w	D_0 ($\times 10^{-7}$), cm^2/s	k_d, mL/g	ref
unannealed EB/NMP solution	230 000	0.0716	19.31	this study
140 °C annealed EB/NMP solution	230 000	0.0553	1.51	this study
Psf[a]/NMP	35 000	1.73	24.6	45

[a] Psf = polysulfone.

ratio of the translational Brownian motion, and frictonal force on a molecular level and k_d is related to solvent quality. k_d can be expressed as[46]

$$k_d = 2MA_2 - k_f - 2\bar{v} \quad (1)$$

where A_2 is the second virial coefficient, k_f is the relative concentration dependence of the frictional coefficient, and $\bar{v}$ the partial specific volume of the solute. For a given molecular weight, k_d decreases smoothly with decreasing solvent quality but passes through a plateau region in the vicinity of the θ condition, where k_d is negative since the virial coefficient will be zero and thus $k_d = -(k_f + \bar{v})$.[47] D_0 of the present EB/NMP samples was about 100 times lower than that of the conventional polymers, probably due to the fact that weight-average molecular weight of EB prepared in this study was 230 000 while that of other polymers are 35 000−50 000 and that EB chains tended to aggregate in NMP. For example, polysulfone (M_w = 35 000) in NMP has a higher D_0 as well as a higher k_d value than EB, indicating that NMP is better solvent for polysulfone, and polysulfone molecules easily fluctuate through the laser beam. For the annealed EB/NMP solution, D_0 and k_d values are smaller than those of EB/NMP unannealed solutions; the movement of EB chain in solution is delayed, and solvent quality decreases with annealing.

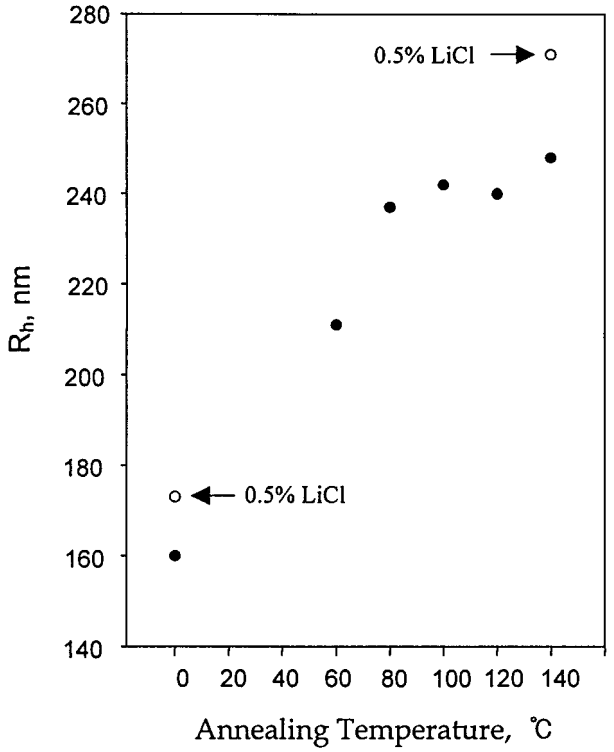

Figure 9. Change of apparent hydrodynamic radius, R_h, with annealing temperature at the 90° scattering angle.

If the EB in NMP solution at 140 °C is reduced to its LB form, the decrease of the number of double bonds due to the protonation in NMP should diminish the stiffness of the backbone and increase the chain flexibility, resulting in a reduction in interchain hydrogen bonding. The net result is a more compact chain with faster D_0.[38] In addition, NMP is a better solvent for LB than EB because amine−amine interchain hydrogen bonding is weaker than imine−amine interchain hydrogen bonding, as confirmed by GPC studies.[21,39] Therefore, the k_d value should increase with the reduction reaction. The small D_0 upon annealing can be assigned to the translational diffusion of large particles composed of many EB molecules by cross-linking reaction. The smaller k_d value is due to the difficulty in dissolving the cross-linked products. Therefore, it is evident that annealing the EB/NMP solution at 140 °C does not cause the reduction, but results in the formation of large particles by a cross-linking reaction, as confirmed by the bimodal autocorrelation function.

The formation of large particles in the annealed EB/NMP solutions was further determined by evaluating the apparent hydrodynamic radius, R_h, using eq 8 at the 90° scattering angle as shown in Figure 9. It was clear from this figure that R_h increased up to 250 nm with the annealing temperature. The reduction of EB chain to LB should result in the decrease of R_h, as reported by Davied et al.,[39] resulting from the chain flexibility and interchain hydrogen-bonding ability as discussed before. The increase of R_h is in good agreement with the decrease of D_0 and R_h of the annealed sample. The effects of LiCl addition on R_h before and after annealing are shown in Figure 9, and the size distributions are shown in Figure 10. As a number of groups have reported, 0.5% LiCl eliminates the aggregation of EB chains, resulting in a narrow molecular weight distribution in GPC.[34,48] After the addition of 0.5% LiCl, R_h of annealed and unannealed samples both

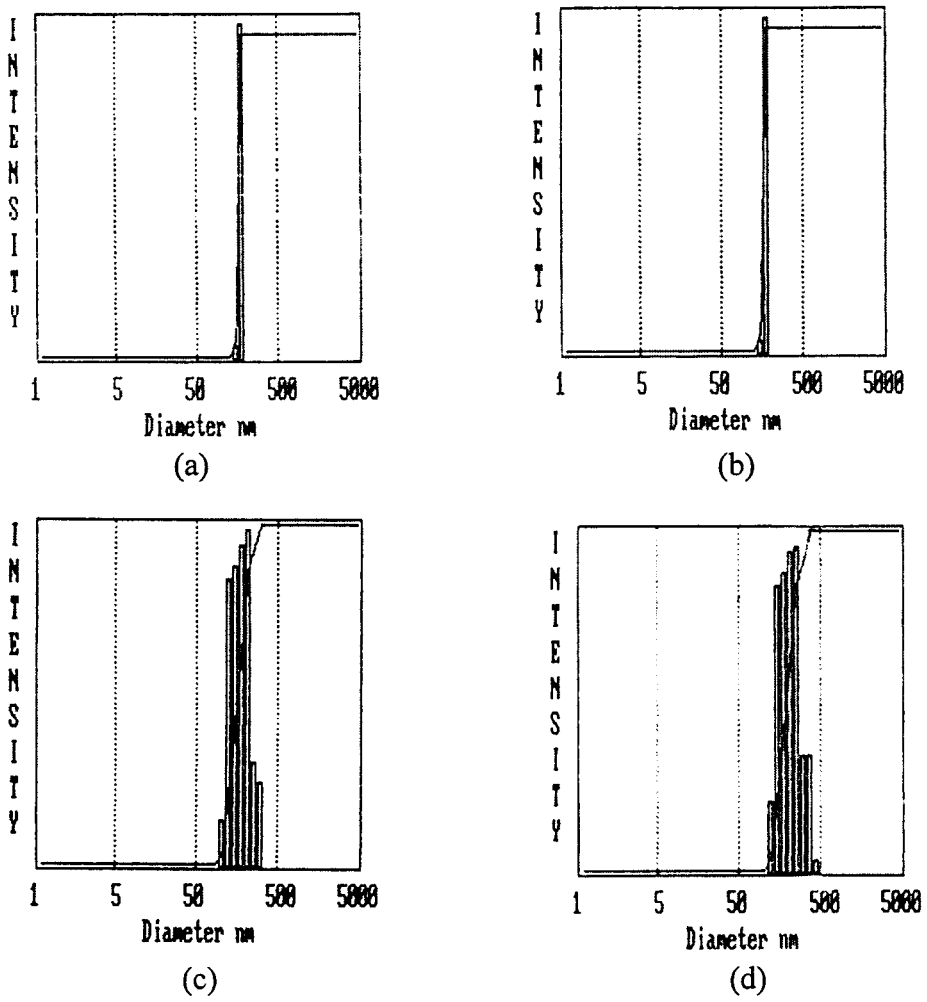

Figure 10. Size distribution profile of (a) unannealed, (b) unannealed after 0.5% LiCl added, (c) annealed at 140 °C, and (d) annealed after 0.5% LiCl added EB/NMP solution.

increased to 173 and 271 nm, respectively. This can probably be attributed to an association between the polar groups of EB and LiCl, resulting in an increase of the overall R_h. The size distribution was broader as the annealing temperature increased and changed little on addition of LiCl. This also confirmed that the increase of R_h was caused by chemical cross-linking, not by physical entanglement or interchain hydrogen bonding. Although it is not possible to compare directly the change of molecular weight before and after annealing because of the absence of GPC data in this dilute region, the combined result of UV−vis, IR, ESCA, and DLS data clearly indicates that the size of EB chains increases, resulting from the chemical cross-linking between EB chains.

Figure 11 shows the concentration dependence of R_h for annealed and unannealed EB chains in NMP. The R_h of annealed EB chains increases with decreasing polymer concentration. The coil expansion at decreasing polymer concentration can be understood as a polyelectrolyte effect; as the concentration of polymer decreases, the ionic strength of solution also decreases, resulting in a decrease of the screening of the charges along the backbone of the polymers. Consequently, the charges along the backbone would be strongly expected to repel each other leading to more expanded polymer chains, as reported by others.[38,40] The yellow color of EB/NMP annealed above 120 °C arises from the fact that EB chains are surrounded by NMP molecules and form

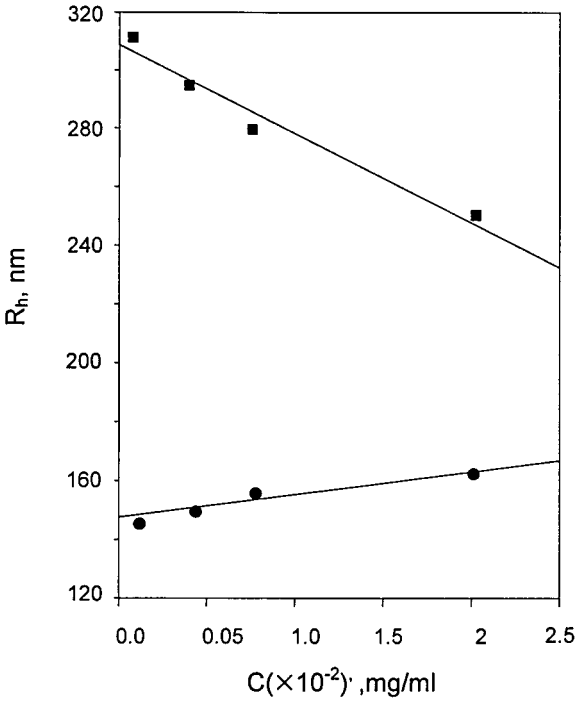

Figure 11. Change of apparent hydrodynamic radius, R_h, with different concentration of (●) EB/NMP and (■) 140 °C annealed EB/NMP solutions at the scattering angle 90°.

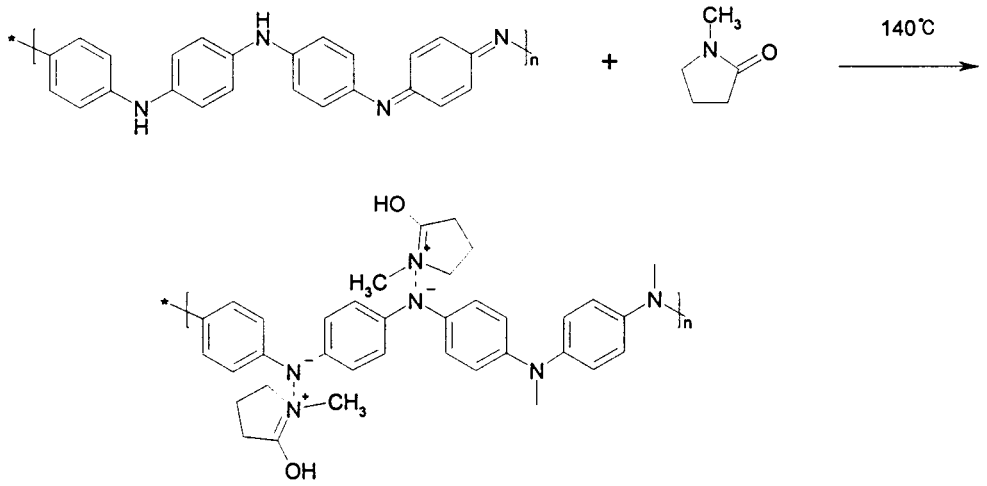

Figure 12. Proposed reaction scheme of EB in NMP at 140 °C.

charge-transfer complexes with NMP. Thus, NMP molecules around EB chains disturb the absorption of light by pure EB chains. On the other hand, for an unannealed sample, R_h slightly decreases with increasing polymer concentration. This is due to the decrease of interchain hydrogen bonding between EB chains as we increase the NMP content.

Figure 12 shows the proposed reaction scheme of EB/NMP at 140 °C. The imine sites of EB chains participate in the cross-linking reaction, as confirmed by UV−vis, FT-IR, ESCA, and DLS results while the amine sites contribute to the formation of the charge-transfer complex with NMP, as evidenced by FT-IR and DLS measurements.

4. Conclusions

The effects of annealing of a dilute EB/NMP solution on changes of chemical and physical properties were investigated. On the basis of the UV−vis, FT-IR, and ESCA measurements, the changes in the chemical property of EB/NMP solutions annealed at 140 °C are as follows. Benzenoid structures and the amine portion increased at the expense of the quinoid structure and the imine portion, respectively. The cyclic N portion also increased. The yellow color of annealed solutions did not change upon the addition of various oxidants.

The changes of physical property of annealed solutions were measured by DLS; the solvent quality of NMP decreased with annealing temperature, as confirmed by the decrease of the mutual diffusion coefficient at zero concentration. The decrease of solvent quality resulted from the formation of large particles or aggregates which was the origin of the slow relaxation mode in the normalized intensity correlation function. The formation of large particles, further confirmed by measuring apparent hydrodynamic radius, is the result of the cross-linked products, in good agreement with UV−vis, FT-IR, and ESCA results. In conclusion, the imine sites of EB chains participated in the cross-linking reaction while the amine sites took part in the charge-transfer complex formation with NMP.

Acknowledgment. Jae Hoon Kim and Jong Seok Kang are grateful to the Institute of Hanyang Brain Korea 21 for a scholarship. This work is supported by the Korea Ministry of Science and Technology under the National Research Laboratory Program in 1999.

References and Notes

(1) Genies, E. M.; Bcyle, A.; Lapkowski, M.; Tsintavis, C. *Synth. Met.* **1990**, *36*, 139.
(2) Stejskal, J.; Krantoshvil, P.; Jenkins, A. D. *Polymer* **1996**, *37*, 367.
(3) Kitani, A.; Yano, J.; Sassaki, K. J. *J. Electroanal. Chem.* **1986**, *133*, 1069.
(4) Angelopoulos, M.; Astuias, G. E.; Ermer, S. P.; Ray, A.; Scherr, E. M.; Macdiarmid, A. G.; Akhtar, M.; Kiss, Z.; Epstein, A. J. *Mol. Cryst. Liq. Cryst.* **1988**, *160*, 151.
(5) Inoue, M.; Navarro, R. E.; Inoue, M. B. *Synth. Met.* **1989**, *30*, 199.
(6) Scherr, E. M.; Macdiarmid, A. G.; Monaohar, S. K.; Masters, J. G.; Sun, Y.; Tang, X.; Druy, M. A.; Glastkowski, P. J.; Cajipe, V. B.; Fischer, J. E.; Cromack, K. R.; Jozefowicz, M. E.; Ginder, J. M.; McCall, R. P.; Esstein, A. J. *Synth. Met.* **1991**, *41*, 735.
(7) Chen, S. A.; Lee, H. T. *Macromolecules* **1993**, *26*, 3254.
(8) Conklin, J. A.; Huang, S. C.; Huang, S. M.; Wen, T.; Kaner, R. B. *Macromolecules* **1995**, *28*, 6522.
(9) Afzali, A.; Buchwalter, S. L.; Buchwater, L. P.; Hougham, G. *Polymer* **1997**, *38*, 4439.
(10) Huang, W. S.; Humphrey, B. D.; MacDiarmid, A. G. *J. Chem. Soc., Faraday Trans.* **1986**, *1*, 82, 2385.
(11) Lee, Y. M.; Ha, S. Y.; Lee, Y. K.; Suh, D. H.; Hong, S. Y. *Ind. Eng. Chem. Res.* **1999**, *38*, 1917.
(12) Briggs, D., Seah, M. P., Eds.; *Practical Surface Analysis*; John Wiley: New York, 1990; Vol. 1.
(13) Shirley, D. A. *Phys. Rev. B* **1972**, *123*, 4709.
(14) Provencher, S. *Comput. Phys. Commun.* **1982**, *27*, 213.
(15) Brown, W.; Johnsen, R. M. *Macromolecules* **1986**, *19*, 2002 and references therein.
(16) Wuld, F. L.; Nowak, F. M.; Heeger, A. J. *J. Am. Chem. Soc.* **1986**, *108*, 8311.
(17) Stafstrom, S.; Bredas, J. L.; Epstein, A. J.; Woo, H. S.; Tanner, D. B.; Huang, W. S.; Macdiarmid, A. G. *Phys. Rev. Lett.* **1987**, *59*, 1464.
(18) Yen Wei, Kesyin, F.; Hsueh, Guang-Way Jang *Macromolecules* **1994**, *27*, 518.
(19) Tang, J.; Jing, X.; Warig, B.; Wang, F. *Synth. Met.* **1988**, *24*, 231.
(20) Show-An, C.; Hsun-Tsing, L. *Synth. Met.* **1992**, *47*, 233.
(21) Zheng, W.; Angelopoulos, M.; Epstein, A. J.; MacDiarmid, A. G. *Macromolecules* **1997**, *30*, 2953.
(22) Bruce, C.; Beard, Spellane, P. *Chem. Mater.* **1997**, *9*, 1949.
(23) Li, Z. F.; Kang, E. T.; Neoh, K. G.; Tan, K. L. *Synth. Met.* **1997**, *87*, 45.
(24) Neoh, K. G.; Kang, E. T.; Tan, K. L. *J. Macromol. Sci., Chem.* **1992**, *A29*, 401.
(25) Neoh, K. G.; Kang, E. T.; Tan, K. L. *Polymer* **1992**, *33*, 2292.
(26) Jeong, B. J.; Lee, J. H.; Lee, H. B. *J. Colloid Interface Sci.* **1996**, *178*, 757.
(27) Han, D. K.; Hubbell, J. *Macromolecules* **1997**, *30*, 6077.
(28) Snauwaert, P.; Lazzaroni, R.; Riga, J.; Verbist, J. J.; Gonbeau, D. *J. Chem. Phys.* **1990**, *92*, 2188.
(29) Demaret, X.; Cristallo, G.; Snauwaert, P.; Riga, J.; Verbist, J. J. *Synth. Met.* **1993**, *55−57*, 1051.

(30) Clark, D. T.; Harrison, A. *J. Polym. Sci., Polym. Chem.* **1981**, *19*, 1945.
(31) Kang, E. T.; Neoh, K. G.; Tan, K. L. *Adv. Polym. Sci.* **1993**, *106*, 135.
(32) Inganas, O.; Salaneck, W. R.; Osterholm, J. E.; Laakso, J. *Synth. Met.* **1988**, *22*, 395.
(33) Kang, E. T.; Neoh, K. G.; Tan, K. L. *J. Polym. Sci., Part A: Polym. Chem.* **1991**, *29*, 759.
(34) Angelopoulos, M.; Liao, Y. H.; Furman, B.; Graham, T. *Macromolecules* **1996**, *9*, 3046.
(35) Zheng, W.; Angelopoulos, M.; Epstein, A. J.; MacDiarmid, A. G. *Macromolecules* **1997**, *30*, 2953.
(36) Tang, X.; Sun, Y.; Wei, Y. *Makromol. Chem., Rapid Commun.* **1988**, *9*, 829.
(37) Adams, P. N.; Apperley, D. C.; Monkman, A. P. *Polymer* **1993**, *34*, 328.
(38) Seery, T. A.; Angelopoulos, M.; Levon, K.; Seghal, A. *Synth. Met.* **1997**, *84*, 79.
(39) Davied, S.; Nicolau, Y. F.; Melis, F.; Rebillon, A. *Synth. Met.* **1995**, *69*, 125.
(40) Gettinger, C. L.; Heeger, A. J.; Pine, D. J.; Cao, Y. *Synth. Met.* **1995**, *74*, 81.
(41) Zhou, Z.; Peiffer, D.; Chu, B. *Macromolecules* **1994**, *27*, 1428.
(42) Fundin, M.; Brown, W. *Macromolecules* **1994**, *27*, 5024.
(43) Jorgensen, E. B.; Hbidt, S.; Brown, W.; Schillen, K. *Macromolecules* **1997**, *30*, 2355.
(44) Shibayama, M.; Fujikawa, Y.; Nomura, S. *Macromolecules* **1996**, *29*, 6535.
(45) Won, J.; Kang, Y.; Park, H.; Kim, U. *J. Membr. Sci.* **1998**, *145*, 45.
(46) Bink, H. *J. Chem. Soc, Faraday Trans.* **1981**, *81*, 1725.
(47) Cotts, P. M.; Selser, J. C. *Macromolecules* **1990**, *23*, 2050.
(48) Liao, Y. H.; Kwei, T. K.; Levon, K. *Macromol. Chem. Phys.* **1995**, *196*, 3107.

MA992004Y